

## Electronic states and optical gain in strained CdS/ZnS quantum structures

U. Woggon, W. Petri, A. Dinger, S. Petillon, M. Hetterich, M. Grün, K. P. O'Donnell,\* H. Kalt, and C. Klingshirn  
*Institut für Angewandte Physik der Universität Karlsruhe, Kaiserstrasse 12, 76128 Karlsruhe, Germany*

(Received 9 September 1996)

Ultrathin, coherently strained CdS layers have been grown epitaxially on ZnS with nominal thicknesses below the critical value for strain relaxation. These CdS/ZnS quantum structures, which show efficient photoluminescence and optical gain in the deep blue to ultraviolet spectral range, have been analyzed with respect to the dimensionality of the electronic states. It has been found that in wide-gap II-VI quantum structures small monolayer fluctuations result in such strong localization of excitons that the localization depth reaches energies around 100 meV. Consequently, the luminescence and gain can well be explained by optical transitions from an ensemble of spatially distributed exciton states in which the deepest and decoupled states can be considered as individual, three-dimensionally confined excitons. [S0163-1829(97)06904-X]

At present, intensive research is being devoted to further lowering of the dimensionality of semiconductor structures from quantum wells toward quantum dots. In III-V-based semiconductor systems, zero dimensionality has been achieved either by lateral nanostructuring of quantum wells or by exploiting the heteroepitaxy of highly lattice-mismatched semiconductors. The technique of self-organized growth has been discovered to obtain regularly shaped, dislocation-free, coherently strained islands, for example in InAs/GaAs structures with 7% lattice mismatch. To explain the optical properties of these nearly uniform islands of nanometer size, a quantum-dot model has been successfully applied.<sup>1</sup> The transfer of such a concept to II-VI materials appears very attractive, in particular in developing low-threshold laser devices made from wide-gap II-VI heterostructures. Zero dimensionality in II-VI quantum structures has very recently been discussed in Refs. 2, 3, and 4 for ZnSe/ZnS,  $(\text{Zn}_{1-x}\text{Cd}_x\text{Se})/\text{ZnSe}$ , and CdSe/ZnSe heterostructures.

Indeed, II-VI semiconductor systems also exist with suitable band offsets and similar strong lattice mismatch like some III-V materials. Thus sufficient strain can be built up in II-VI layers of a few monolayers thickness; however, the occurrence of the Stranski-Krastanow growth mode depends critically also on surface energies of the involved materials and on the growth conditions. Only little is known about the surface energies in II-VI materials, but the usually low growth temperatures compared with III-V heteroepitaxy do not favor processes driven by thermal equilibrium like strain-induced islanding. Furthermore, II-VI compounds show smaller reduced shear moduli due to their higher ionicity.<sup>5</sup> Plastic relaxation therefore may also beat elastic relaxation by islanding in those cases where the surface energy situation favors the latter. Hence strong lattice mismatch does not inevitably result in strain-induced islanding in II-VI materials. The characteristic feature of the deposited layers could also be a large interface roughness. Monolayer fluctuations on length scales comparable to the excitonic Bohr radius, however, should likewise be able to confine excitons spatially, and thus offer an alternative route towards zero dimensionality. Three-dimensional confinement of electronic states has distinct consequences for gain processes in quantum

structures. A spectrally broad gain region is expected, owing to the inversion of a multitude of discrete one-pair transitions and contributions from the stimulated decay of two-pair states, as recently shown in Ref. 6. When the zero dimensionality of electronic states is caused by localization in a variety of different local potentials, the absolute value of the gain at a certain energy is determined by the density of energetically equivalent confinement potentials. Thus the gain spectrum measured for the whole sample can significantly differ from that of the individual dots.

To study the electronic properties of such highly strained II-VI semiconductor systems, we have chosen the material combination CdS/ZnS with a lattice mismatch of 7.3%. Because of their band-gap energies ( $E_{\text{gap}} = 2.58$  eV for CdS and 3.83 eV for ZnS), CdS/ZnS-based heterostructures with two-dimensional or even stronger quantum confinement have the potential for emission in the deep-blue to ultraviolet spectral range. Since currently only a few II-VI-based materials are known which emit in the spectral range  $< 450$  nm, zero-dimensional CdS/ZnS quantum structures might open a way to the shortest emission wavelength that can be realized by wide-gap II-VI semiconductor heterostructures.

Two different samples grown on a (001) GaAs substrate are discussed here. Sample 1 consists of ten periods of an ultrathin CdS layer with an average thickness of 3 ML separated by 19-nm-thick ZnS barriers grown onto a thick ZnS buffer. This sample has been grown by compound source molecular-beam epitaxy at  $T_{\text{subst}} = 190$  °C. Sample 2 has a structure similar to sample 1 but with thinner ZnS barriers ( $L_B = 3$  nm) and 100 periods of CdS/ZnS, and is obtained from metalorganic chemical vapor deposition at  $T_{\text{subst}} = 300$  °C. Transmission electron microscopy (TEM) showed a complete wetting of the ZnS surface by CdS without extra defect generation at the interface, i.e., coherently strained layers. The measured values for the film thickness confirm the values adjusted via the growth rate of  $\sim 3$  ML or less ( $\leq 1$  nm). This thickness lies below the critical thickness value for strain relaxation of 4–5 ML.<sup>7,8</sup> High-resolution images of our samples, however, indicate interface roughness and marked thickness fluctuations. The information obtained by TEM and even high-resolution TEM is not sufficient to identify unambiguously the spatial profile of the CdS layer,

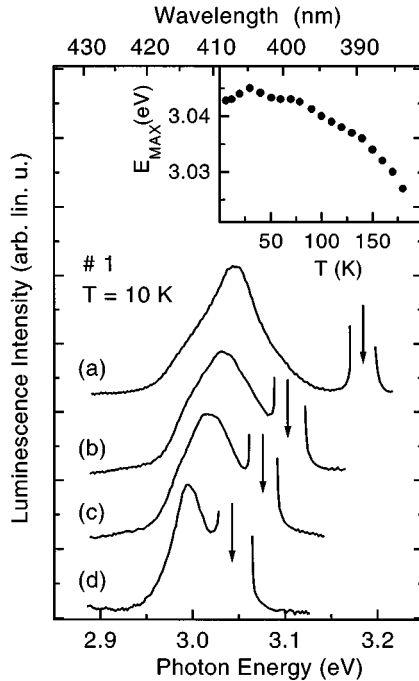


FIG. 1. Photoluminescence of the ten-period CdS(1 nm)/ZnS(19 nm) quantum structure (sample 1) for different excitation energies above resonant (a) and on-resonant (b)–(d). The inset shows the shift of the peak energy of spectrum (a) as a function of temperature.

both within the CdS plane and in the growth direction. Neither islands nor regular layers could be favored as the characteristic feature of the samples. To figure out the properties of the grown structures, in the following we will analyze the luminescence properties. We will show that we can identify by means of optical methods the degree of confinement in the coherently strained CdS/ZnS quantum films. Measuring the gain spectrum, we find gain in the spectral range around 3.0 eV with spectrally broad characteristics and values for the sample gain around  $100\text{--}250\text{ cm}^{-1}$  up to temperatures of  $T=160\text{ K}$ .

To discuss the dimensionality of electronic states in epitaxially grown structures, we consider three different situations: (a) The case of an ideal two-dimensional structure, i.e., a quantum well or superlattice is grown with uniform layer thicknesses in the range of a few ML's. If monolayer fluctuations exist, they only occur over distances large compared to the bulk Bohr radius. Other types of interface roughness shall only result in larger homogeneous line broadening, since the excitonic wave function may average over these local potential fluctuations. (b) The case of an ensemble of nearly identical, isolated quantum dots which are grown in a self-assembled growth mode and have nearly the same energy states (appropriate for the description of strain-induced pyramidal islands such as in the InAs/GaAs system). (c) The case of randomly distributed, local potentials which localize excitons to such an extent that they form single quantum dots, but with very different, individual energies (similar to localized states at monolayer fluctuations in quantum wells or at composition fluctuations in mixed crystals). These limits exhibit typical optical properties which can be distinguished in optical experiments. Description (a) or (b) can be

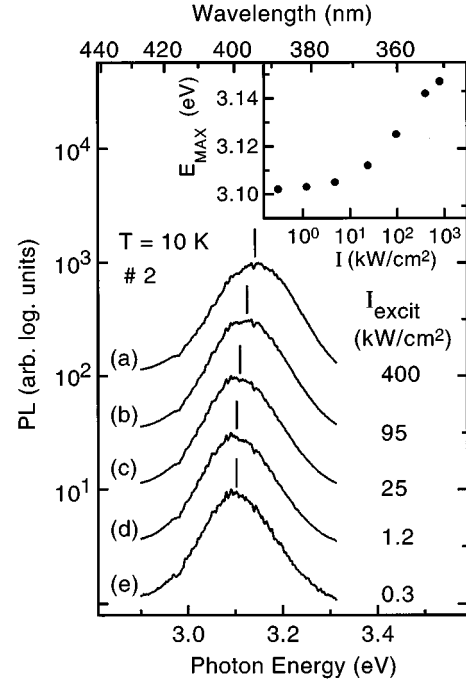


FIG. 2. Photoluminescence of the 100-period CdS(1 nm)/ZnS(3 nm) quantum structure (sample 2) as a function of excitation intensity. The inset shows the shift of the peak maximum as a function of pump intensity.

favored when observing strictly size-correlated energy shifts to higher values compared to the bulk when decreasing the well thickness or the pyramid size. In time-resolved experiments, we expect a spectrally uniform decay of a dominantly homogeneously broadened line. With increasing intensity, subsequent filling of the excited states results in the appearance of high-energy peaks at fixed energy positions defined by the confinement potential. Case (c) represents the extension of the conventional model for localized states towards zero dimensionality. Discrete energies and a  $\delta$ -like density of states are characteristic of deep localized, decoupled states within a potential landscape. Excitons in these states are not able to tunnel to the next potential minimum during their lifetime at a given temperature, and form the exponential tail in the density of states. They appear in the spectra redshifted with respect to the energy of the corresponding extended states. Case (c) dominates if we observe a strong inhomogeneously broadened luminescence line, a high sensitivity of the line shape to temperature changes (thermally activated multiple trapping may lead even to blueshifts of the line maximum with increasing temperatures), and a nonuniform decay behavior within the spectrum due to the motion of excitons between the different potential minima.

Figure 1 shows the cw photoluminescence of sample 1 measured at different excitation energies and temperatures. Excitation above the resonance [spectrum (a)] yields a highly efficient luminescence band at 3.045 eV with a half-width of 80 meV. The deviation of the spectral shape from a Gaussian, typically found in strong inhomogeneously broadened systems, is caused by a weak modulation of the spectra by Fabry-Perot modes. The photoluminescence of sample 2 at comparable excitation conditions is shown in Fig. 2 [spectrum (e)]. We note that both samples show similar peak en-

ergies, although in sample 1 the CdS layer is separated by thick ZnS barriers, and in sample 2 by very thin ZnS barriers. Thus, supposing the dominance of case (a), the energies should be different for the quantum-well-type sample (sample 1) and the superlattice-type sample (sample 2). Moreover, two or three sharp lines are expected in the luminescence spectra according to well thicknesses of 2, 3, or 4 ML, in particular for the quantum-well-type sample 1. Thus, we cannot favor case (a) to explain the electronic states in the strained CdS/ZnS quantum structures investigated here.

To study the homogeneous or inhomogeneous character of line broadening, the excitation energy is tuned continuously into the resonance [spectra (b)–(d) in Fig. 1]. All contributions to the luminescence signal above the excitation energy disappear, and the linewidth decreases, i.e., the luminescence band is strongly inhomogeneously broadened. The temperature dependence of the peak energy (inset), measured for spectrum (a) shows a nearly constant value with increasing temperature up to  $\sim 90$  K. This temperature behavior distinctly deviates from the temperature-dependent shift of the *A*-exciton energy measured for a CdS platelet in the same temperature range. The absence of the usual  $dE_{\text{gap}}/dT$  dependence known from the bulk shows that thermal activation of phonon-assisted detrapping is possible within the grown structure, resulting in a population of local potential minima with a lower localization depth. The result is a spectrally roughly constant luminescence peak due to the compensation of that blueshift with the redshift of the gap energy. The features observed can well be understood in the context of case (c) of the three limits discussed above. Therefore, the quenching in the luminescence efficiency with increasing temperature has been studied (not shown here) to obtain an estimate for the localization depth, supposing that the thermally activated mobility of the carriers is connected with a higher nonradiative decay rate. Considerable luminescence has been detected up to room temperature. By fitting the temperature-dependent luminescence quenching with an Arrhenius-type model,<sup>9</sup> an activation energy of 70 meV has been determined. From this measurement and from the value of inhomogeneous broadening (between 80 and 150 meV), we conclude that the localization depth is huge and reaches energies in the  $\approx 100$ -meV range, which clearly exceeds thermal energies, even at room temperature.

Figure 2 shows the intensity dependence of the luminescence measured for sample 2 (but similarly found also in sample 1) by pumping above the resonance with a nitrogen laser-pumped dye laser. In case (a) or (b) discussed above, population of the next, higher excited pair state (which is defined by the confinement resulting from the quantum well or pyramid size and is well separated in energy) would lead to a second peak in the luminescence. Instead, we observe a blueshift of the peak maximum of the whole luminescence band and a line broadening which can only well be understood in the context of case (c). The same statement holds for the time dependence of the luminescence decay. Figure 3 shows the time decay of the photoluminescence measured by a streak camera after excitation with 70-ps pulses at 250 nm for low and high excitation intensities. The spectrally different decay times in Fig. 3(a) with the tendency of longer decay on the low-energy side of the spectrum indicate coupling between the localized states, and transfer between them

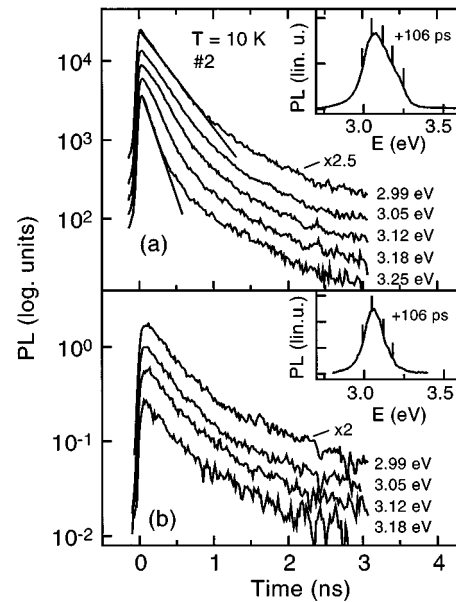


FIG. 3. (a) Decay of photoluminescence of the 100-period CdS(1 nm)/ZnS(3 nm) quantum structure (sample 2) at selected energies within the spectrum shown in the inset (taken at a fixed delay of +106 ps). The excitation fluence is  $4 \text{ mJ/cm}^2$ . (b) The same as (a), but for a fluence of  $40 \mu\text{J/cm}^2$ .

for the highest excitation intensity used in the experiment. Likewise, we observe a redshift of the peak maximum and a decrease of the linewidth with time due to relaxation processes within the different potential minima. At very low excitation [Fig. 3(b)] only the energetically lowest states are filled by the pump, and the decay becomes more uniform within the luminescence band. Apparently, after relaxation into the deep localized states, the excitons are decoupled, and transfer between the different sites is no longer possible.

To resolve these individual, decoupled excitons, spectrally we decreased the excitation spot down to  $2 \mu\text{m}$ , but the spectra remain unstructured and no single sharp lines have been observed. Therefore, we conclude that the density of these localized states is very high. If we assume a random distribution of localization centers over a spot size of  $\sim 1 \mu\text{m}$ , an inhomogeneous broadening of some tens of meV and a linewidth of  $\sim 1 \text{ meV}$ , then already a density of  $10^3$ – $10^4$  states is enough to smear out the optical spectra.

The experimental results of Figs. 1–3 clearly show that luminescence from excitons, localized in randomly distributed potential minima, dominates the optical properties of the CdS/ZnS structures. The description of our structures according to case (c) has distinct consequences for the gain spectrum, as demonstrated in Fig. 4. The gain is measured for sample 1 by the variable stripe length method with the nitrogen laser as pump source ( $E_{\text{exc}} = 336 \text{ nm}$ , maximum power  $2 \text{ MW/cm}^2$ ). Figure 4 demonstrates the occurrence of optical gain in the spectral range around 3.0 eV. The gain spectrum is spectrally broad, and stretches about 200 meV toward lower energies. Two factors contribute to the spectral broadness of the gain: the contribution from differently localized excitons (gain from an ensemble of individual quantum dots with different energies) and the contribution from different gain processes within the single dot, like stimulated

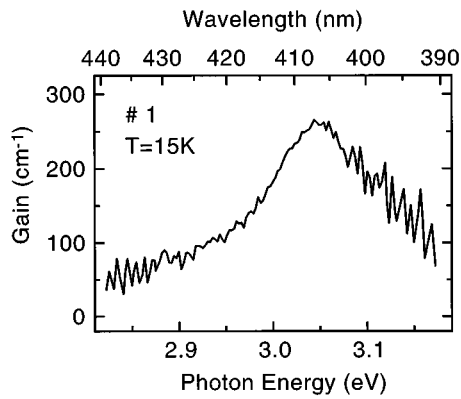


FIG. 4. Spectrum of the optical gain measured at the ten-period CdS(1 nm)/ZnS(19 nm) quantum structure (sample 1) and at  $T=10$  K,  $I_{\text{exc}}=2$  MW/cm<sup>2</sup>, and  $\hbar\omega_{\text{exc}}=3.68$  eV.

processes arising both from one- and two-pair states. The gain spectrum of the whole sample is composed from a variety of different gain processes. Even when the single dot is characterized by a large, spectrally sharp gain and low threshold behavior, the *sample* gain can remain small, and

can be distributed over a broad spectral range. On the other hand, the existence of a continuum of extended states at higher energies and with high density of states can be used for optical pumping because of its efficient photon absorption. This provides a high number of excited electron-hole pairs which then build up the inversion in the system of localized states.

To summarize, we report the growth of ultrathin, coherently strained CdS/ZnS quantum structures which emit very efficiently in the spectral range around 400 nm. A study of the luminescence properties and the optical gain shows that the consideration of discrete states confined by local potentials and forming individual quantum dots describes the zero dimensionality of electronic states in highly strained, lattice-mismatched II-VI heterostructures. Because in our system thickness fluctuations in the monolayer range result in energy changes on the 100-meV scale, the roughness of the structure itself is sufficient to provide quantum confinement, and to produce individual quantum dots.

The authors are grateful to D. Gerthsen and the Laboratorium of Electron Microscopy of the University of Karlsruhe for TEM measurements. This work was supported by the Deutsche Forschungsgemeinschaft.

\*Permanent address: Department of Physics, University of Strathclyde, Glasgow, Scotland.

<sup>1</sup>M. Grundmann, O. Stier, and D. Bimberg, Phys. Rev. B **52**, 11 969 (1995), and references therein.

<sup>2</sup>Yi-hong Wu, K. Arai, and T. Yao, Phys. Rev. B **53**, R10 (1996); **53**, 485 (1996).

<sup>3</sup>M. Lowisch, M. Rabe, B. Stegemann, F. Henneberger, M. Grundmann, V. Türck, and D. Bimberg, Phys. Rev. B **54**, R11074 (1996).

<sup>4</sup>V. Nikitin, P. A. Crowell, J. Levy, F. Flack, N. Samarth, and D. D. Awschalom (unpublished).

<sup>5</sup>R. M. Martin, Phys. Rev. B **1**, 4005 (1970).

<sup>6</sup>H. Giessen, U. Woggon, B. Fluegel, G. Mohs, Y. Z. Hu, S. W. Koch, and N. Peyghambarian, Opt. Lett. **21**, 1043 (1996).

<sup>7</sup>P. J. Parbrook, B. Henderson, K. P. O'Donnell, P. J. Wright, and B. Cockayne, J. Cryst. Growth **117**, 492 (1992).

<sup>8</sup>G. Brunthaler, M. Lang, A. Forstner, C. Giftge, D. Schikora, S. Ferreira, H. Sitter, and K. Lischka, J. Cryst. Growth **138**, 559 (1994).

<sup>9</sup>F. Yang, P. J. Parbrook, C. Trager, B. Henderson, K. P. O'Donnell, P. J. Wright, and B. Cockayne, Superlatt. Microstruct. **9**, 461 (1991).